# P9.2 THE USE OF KITE OBSERVATIONS TO STUDY AIR-SEA INTERACTION-CONTROLLED ATMOSPHERIC SURFACE LAYER PROFILES DURING THE RED EXPERIMENT

Kenneth L. Davidson[1], Peter S. Guest[1], Deborah L. Mabey[1], Paul A. Frederickson[1], Kenneth D. Anderson[2]

[1]Naval Postgraduate School, Monterey, CA
[2]SPAWAR Systems Center, San Diego, CA

## 1. INTRODUCTION

The Roughness and Evaporation Duct (RED) experiment was designed to relate the effect of atmospheric boundary layer (ABL) features as well as ocean surface roughness to near-surface high frequency electromagnetic propagation. For this, ABL and ocean surface data, as well as propagation data, were collected at mid-path locations in August and September 2001 off the windward coast of Oahu, Hawaii. The Naval Postgraduate School (NPS) and SPAWAR Systems Center, San Diego (SSC-SD) performed collaborative atmospheric surface layer (NPS) and propagation (SSC-SD) measurements to identify the state of understanding of the atmosphere influence.

Air-sea interaction processes determine atmospheric surface layer properties that include the gradients as well as the fluxes. The vertical gradient of the modified index of refraction (or modified refractivity), M, is important in the propagation of UHF, VHF and microwave frequencies immediately above the sea. M depends on three atmospheric parameters: pressure (p), temperature (T), and the partial pressure of water vapor (e). Of these three, temperature and vapor pressure (humidity) are most significant and have variations that must be accounted for by measurements and modeling. Gradients of humidity near the surface over ocean regions usually cause radio waves at frequencies greater than approximately 3 GHz to be trapped in the atmospheric surface layer, a phenomenon called evaporation ducting. Since these gradients cannot normally be measured precisely near the surface, bulk methods (Fairall et al, 1996) based on air-sea interaction processes and single level and surface measurements are used to approximate the profile of M. The purposes of this study utilizing NPS collected data are: 1) to evaluate bulk methods by measuring profiles of p, T and e directly using a buoy and a kite flown from a mobile platform; 2) to evaluate the impact of differences between the bulk and directly-measured profiles on radio frequency (RF) propagation using the Advanced Refractive Effects Prediction System (AREPS) program, and 3) to compare AREPS predictions based on bulk and directly-measured profiles with observed loss values. A fuller discussion of the methods and results presented in this study can be found in Mabey (2002).

*Corresponding author address: Kenneth L. Davidson, Department of Meteorology, Naval Postgraduate School, 589 Dyer Road, Room 254, Monterey, CA 93943-5114; e-mail: davidson@nps.navy.mil

## 2. THE BULK METHOD

The air-sea interaction-controlled atmospheric boundary layer (ABL) properties of primary interest in RED were the profiles, because the refractivity profile immediately above the surface affects radar surface clutter return as well as detection range and the temperature profile is responsible for optical turbulence and mirages. The bulk method used to estimate refractivity profiles is based on applications of flux-profile relationships for vertical gradients of temperature ($\frac{\partial T}{\partial z}$) and specific humidity ($\frac{\partial q}{\partial z}$) in the surface layer and depends on scaling parameters that are related to the turbulent vertical fluxes of momentum, sensible heat and latent heat (moisture). When turbulent fluxes are not measured directly, the scaling parameters can be determined using measurements of temperature ($T_s$) at the surface (humidity at a sea water surface is assumed to be 98% of the pure water saturation humidity value), as well as temperature, humidity and wind speed at some reference height, z, which must be near (within approximately 20 m of) the surface.

Important to the bulk method are the empirically derived functions and constants, the Monin-Obukhov Similarity (MOS) theory stability function ($\psi$), and the roughness length ($z_{oT}$). The expressions for temperature, with similar equations for surface layer humidity and wind speed profiles, are as follows (where parameters subscripted with asterisks are scaling parameters), $\kappa$ is the von Karman constant (0.4), $g$ is the acceleration of gravity, and $L$ is the Obukhov length scale.

$$T_* = (T_z - T_s)\kappa[\ln(\frac{z}{z_{oT}}) - \psi_T(\xi)]^{-1} \quad (1)$$

$$\xi = \frac{z}{L} \tag{2}$$

$$L = \frac{T_v u_*^{\,2}}{\kappa g (T_* + 0.61 T q_*)} \tag{3}$$

The scaling parameters determination enable gradients to be calculated using equations similar to the equation for the temperature gradient, $\frac{\partial T}{\partial z} = \frac{T_*}{\kappa z}\Phi(\frac{z}{L})$, where $\Phi$ is a stability function determined experimentally over land (Fairall et al, 1996). Time-averaged surface and reference height variables are commonly known as bulk parameters and thus the profiles of T, q and M derived in this manner are called bulk profiles.

## 3. ATMOSPHERIC AND OCEAN SURFACE DATA COLLECTION AND PROCESSING

Two sets of measurements from two different platforms formed the basis of mid-path descriptions of ABL properties that could affect near-horizon microwave propagation. One set consisted of mean and fluctuating air and sea properties from a buoy positioned along the electro-optical (EO) path and the other consisted of the vessel single level and kite-borne mean air properties from the R/V *Wailoa*, which traversed both the EO and RF paths (Fig. 1). The data collected from both the NPS buoy and the vessel-based kite sensors are shown in Fig. 2 as a time series of the buoy data and by the number of kite profile collections shown in the top panel.

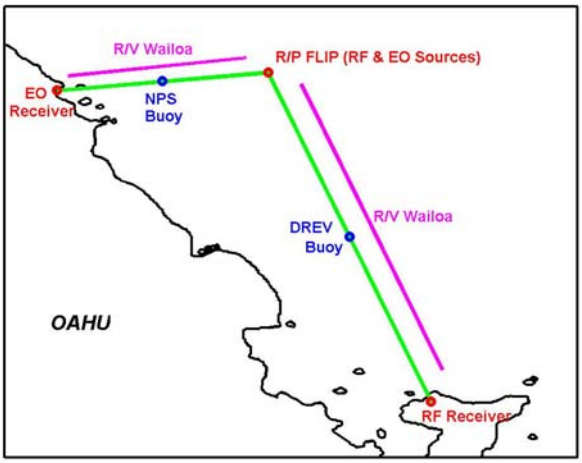


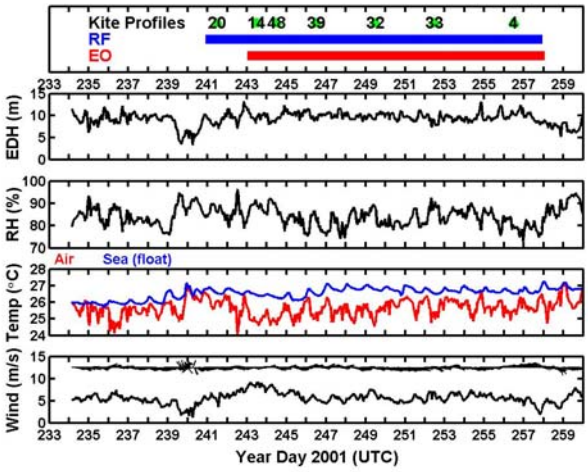


**Figure 2.** Time series of NPS Flux Buoy data and kite profile collection times. Top panel: Kite profile collection times and number of profiles collected; Second panel: Evaporation duct height; Third panel: Relative humidity; Fourth Panel: Air temperature shown in red, sea temperature shown in blue; Bottom panel: Wind speed shown by black line, wind direction indicated by barbs at top of panel.

The deployed NPS buoy system (Fig. 3) collected atmospheric surface layer and ocean surface data continuously from August 22, 2001 0240 UTC until September 18, 2001 1554 UTC, Frederickson et al. (2003). Buoy sensors

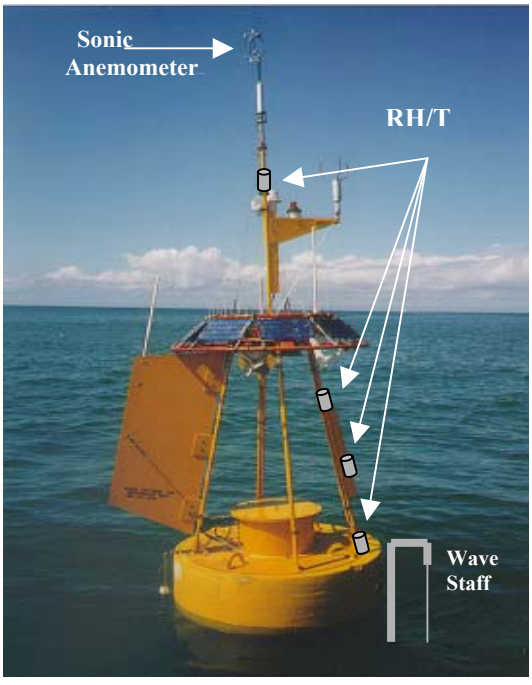


**Figure 3.** Photograph of the NPS Flux Buoy showing locations of the sonic anemometer, relative humidity/temperature profile sensors, and wave staff.

measured pressure at 0.4 meters above the surface, wind speed and wind direction at 4.15 meters, and air temperature and relative humidity at 0.71, 1.04, 2.06 and 4.08 meters. Sea surface temperature measurements were made at 1.2 meters below the surface and at the surface using a floating thermistor and with an infrared (IR) radiometer. Results described here are based on the IR sea surface temperature in calculating bulk profiles.

A kite-borne radiosonde with receiver system enabled the measurement of profiles of pressure, temperature and vapor pressure from near the surface (<1 m) to the top of the surface layer (approximately 100 m). The kite-borne radiosonde profile collection method was selected because it enabled descriptions to levels above the evaporation duct. However, the collection could also be applied to evaluation of temperature and humidity profile scaling. In the kite-borne system, an approximately ten-meter length of 50-pound test kite string was attached to either a four-foot or six foot nylon delta kite as shown in Figs. 4 and 5. The 500 feet of kite string was on a reel attached to a salt-water fishing rod that was secured to the side of the boat. During the process of rigging and launching the kite, a Vaisala RS-80 radiosonde was prepared and activated for manual launch.

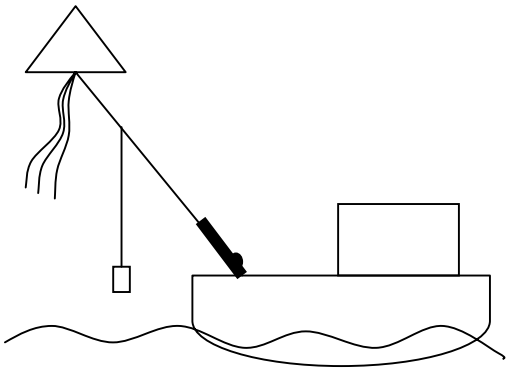

**Figure 4.** Schematic drawing of the NPS kite profiling system.

Hand-exerted pressure on side of the reel controls the kite's horizontal movement away from the vessel while maintaining the sonde's height above the sea surface of approximately one meter. Once the kite-borne radiosonde had reached a distance of approximately 50 to 100 meters away from the ship, the kite was caused to rise by restoring full drag to the real. The kite was reeled in until the radiosonde was approximately one meter from the side of the ship. The process was repeated until the time

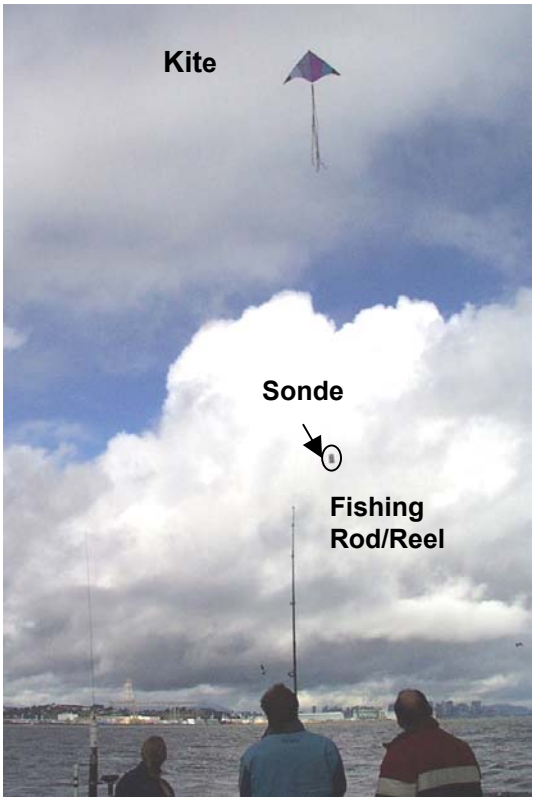


**Figure 5.** Photograph of a kite-sonde profile being measured from a research vessel.

limit of data collection (two hours) was reached. In this manner, approximately fifteen to 25 up-down kite profiles were obtained during each two-hour data collection session. The Vaisala RS-80 radiosonde transmitted measured values of temperature, pressure and vapor pressure every two seconds during the up-down excursions. It has accuracy, and resolution of 0.5 hPa/0.1 hPa for pressure and accuracy/resolutions/response times of 0.2 C/0.1 C/2.5 s, and 2%/1%/1 s for Temperature, and humidity, respectively.

The buoy sensor data were averaged over one-minute intervals. The kite-borne radiosonde collected data had several specialized processing procedures developed specifically for this application. The kite data had to be edited and formatted into an acceptable form for analysis and display. First, bad data (generally due to receiving a signal from another radiosonde) were removed and missing data were noted. Second, heights corresponding to the measured data had to be assigned since features of interest were detail profiles. To establish heights of the kite-borne radiosonde data, hydrostatic balance was assumed. It was further assumed that the kite-borne sonde reached a minimum elevation of one meter each time it left the vessel. Subjective interpretations

of the pressure time series were made to determine the points where the kite left the ship and where it returned (see Fig. 6). During each of these periods (which lasted approximately five minutes), the minimum height was adjusted to one meter and all other heights were adjusted by the same amount. These time series were also used in determining the extent of the vessel contamination envelope.

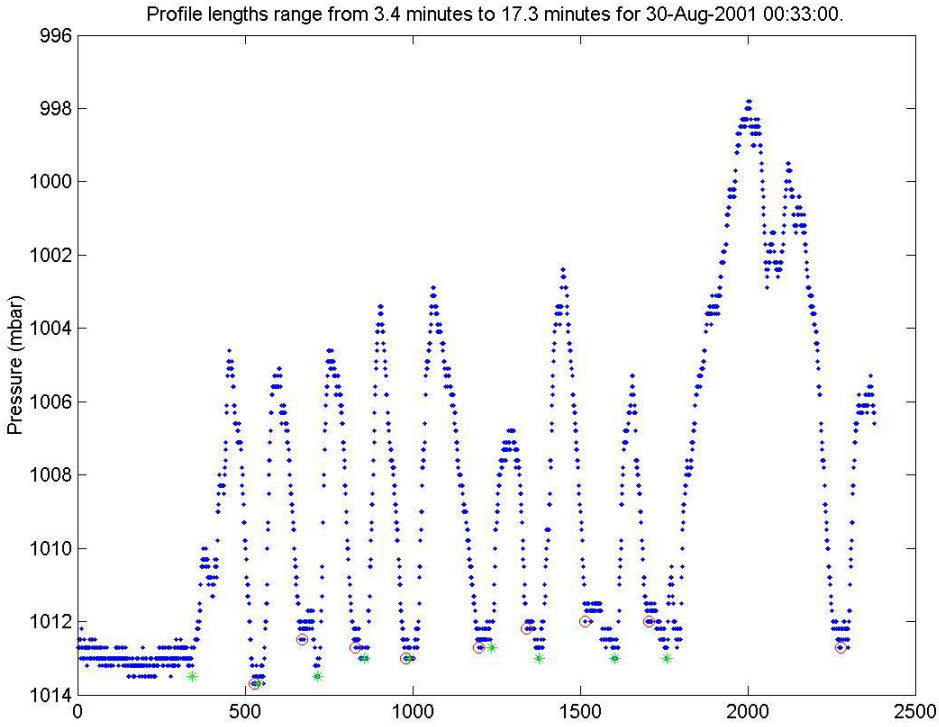


**Figure 6.** Example of a radiosonde-measured pressure time series, showing the manual selection of starting and stopping points for each kite up/down profile, indicated by red and green circles.

The kite obtained records were divided into sampling periods which were approximately 20 to 40 minutes in duration. For each sampling period, profiles were determined on the basis of bulk calculations as well as direct profile measurements. For the kite profile descriptions, data were grouped within height bins for averaging. Below 32 meters, the kite data bin consisted of 1-meter deep levels and from 35 to 100 meters, the kite data bins consisted of 5-meter deep levels. For the buoy profile, humidity and temperature data were collected at 0.71 m, 1.04 m, 2.06 m and 4.08 m and buoy pressure data at 0.39 m.

Comparisons of refractivity profiles will be the emphasized ABL feature. For both the kite and the buoy temperature, humidity and pressure data, refractivity values were calculated using the following equation:

$$M = 77.6\frac{p}{T} - 5.6\frac{e}{T} + 375000\frac{e}{T^2} + 0.157z \quad (4)$$

Regression analyses were preformed on the kite-measured data to obtain comparative profiles. In most cases, the bin averaged M values at the lowest two levels (1.5 and 3.5 meters) from the kite data were too low. The profiles did not exhibit the expected strong humidity gradient. This feature and the fact that these low level values were not in agreement with the buoy measurements suggested that there was an error in the lowest level kite values. For this reason, kite derived values below 3.5 meters were not used in regression fits.

The bulk model derived profiles were based on mean airflow parameters adjusted to the 19.5-meter level for the kite for comparison with the kite direct measurements and from the mean airflow measurements at 4.08 meter level on the buoy for comparison with the buoy profile. The vessel bucket and the buoy IR sea surface temperatures were used in both cases. The bulk model functions and associated calculation

procedures are described by Frederickson et al. (2003).

## 4. RESULTS

### 4.1 *Direct and bulk model Profiles*

The results of kite-buoy measurements and bulk model comparisons will emphasize the refractivity profile, although interpretation could also be made on with the temperature and humidity profiles. As illustrated In Fig. 7, the kite refractivity values were usually ~10 M-units lower than the buoy values. Henson (2002) recently suggested that the RS-80 humidity sensor can develop a dry bias while stored for as little as three to four months. Hence, the kite values were adjusted to match with the buoy values using quadratic function fits from the kite data only and the buoy data only. The mean difference between the two polynomials for the region between the top buoy value and the bottom kite value was used to adjust all kite values, as indicated in Fig. 8. Comparison of a typical merged and bulk profile set appears in Fig. 9.

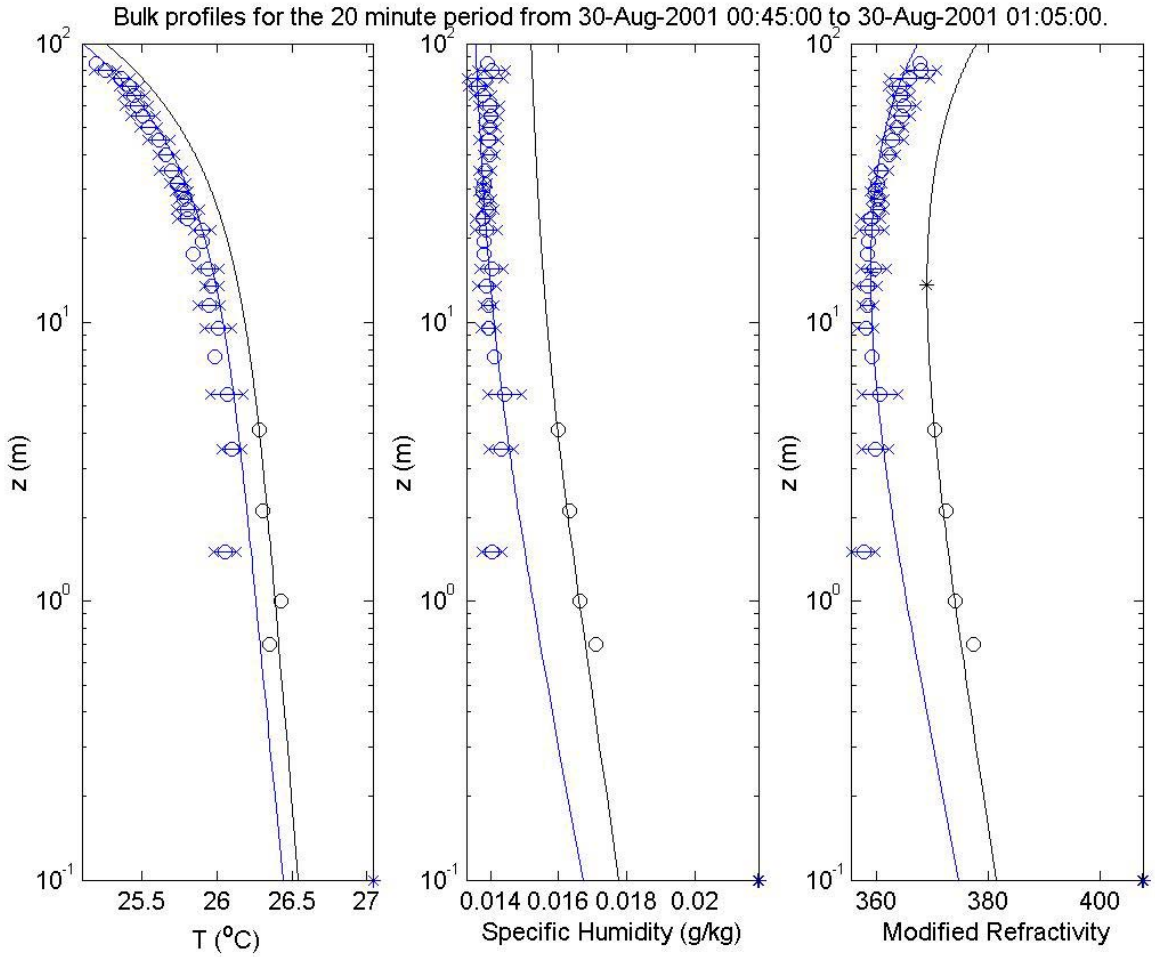


**Figure 7.** Profiles of temperature, specific humidity and modified refractivity versus height (log scale). Black circles are buoy data. Blue circles are kite-borne radiosonde data. Bars associated with blue circles represent plus and minus one standard deviation. Blue circles without associated bars are averages of less than ten data points. Solid lines are bulk profiles. The black solid line is computed from the 4.08-meter buoy data. The blue solid line is computed from the 19.5-meter kite-borne radiosonde data.

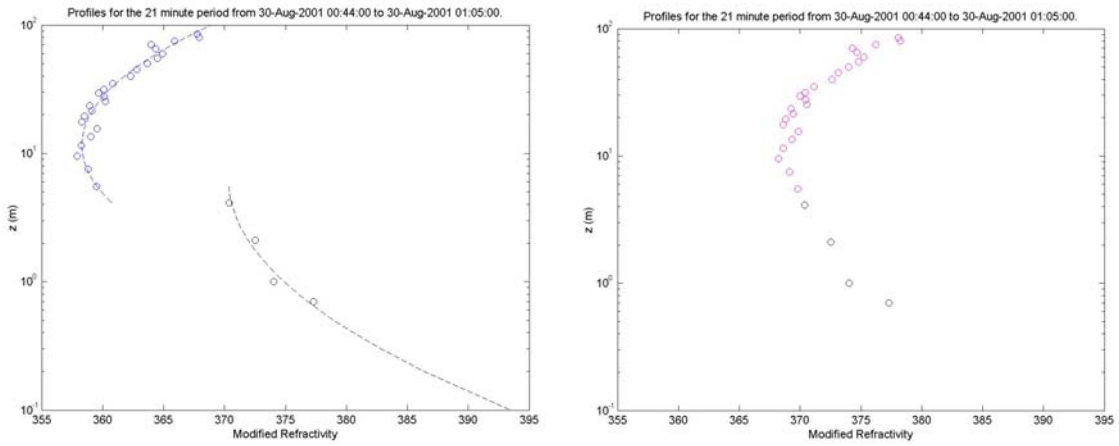


**Figure 8.** The left panel shows actual kite-borne radiosonde data (blue circles) and buoy data (black circles) with quadratic functions fit to them. Right panel shows the same buoy data with the adjusted kite-borne radiosonde data (magenta circles).

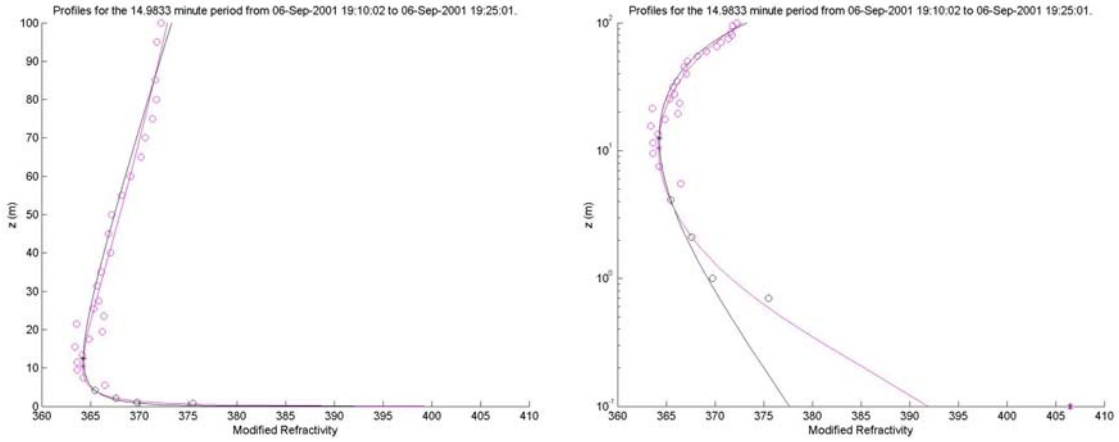


**Figure 9.** An example (linear height scale on the left, log on the right) of a case when the bulk profile from the buoy data (black line, procedure described below) and the smoothed profile from the kite-borne radiosonde data merged with the buoy data (magenta line) matching well above 3.5 meters.

A data set was developed to obtain an overall measure of the deviations of observed from bulk derived refractivity profiles. The combined buoy data (including the surface value based on the infrared sea surface temperature) and kite-borne sonde derived data from (5.5 meters to 100 meters) were fit to the natural logarithm of height with a quartic function. The buoy profile data alone could not be used to create a reasonable smoothed profile of M up to the evaporation duct height. Since the evaporation duct height (the height of the minimum value of M) generally occurred above four meters, any polynomial fit to the four buoy data points would be monotonically decreasing with height, which is unrealistic. The generated bulk profiles from the buoy data used the same averaging periods as the smoothed results. The temperature and relative humidity values from 4.08 meters, in addition to the pressure and wind speed data, were used with the bulk model described above.

Regarding the comparison of bulk and smoothed profiles, differences between the slopes of the modified refractivity profiles, not the values themselves, are important in determining propagation. Results from comparison of bulk and smoothed profile slopes are in Figs 10 (blue lines) for different regions above the surface. In general, slopes of the two types of profiles are in good agreement above 3.5 meters; the

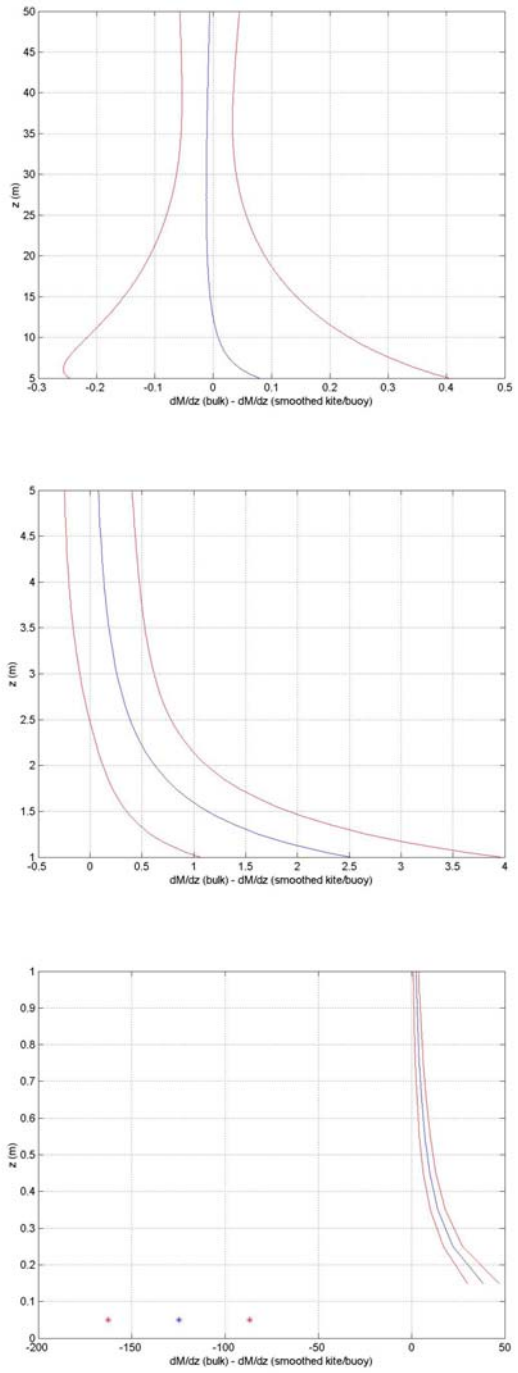


**Figure 10.** Blue lines represent the mean difference between the first order approximations of dM/dz (45 averaging periods). Red lines represent plus and minus two standard deviations. Top panel is from five to 50 meters; center panel is from one to five meters; bottom panel is from the surface to one meter. Asterisks are used to designate the 0.05-meter values.

differences in both value and gradient are well within one standard deviation of zero. Below 3.5 meters, except in the lowest ten centimeters, the smoothed profiles exhibit stronger negative gradients than the bulk profiles (differences noted peaked at 38 $M \bullet m^{-1}$). Conversely, the bulk profile has an extremely strong negative gradient in the lowest ten centimeters (the mean difference was 125 $M \bullet m^{-1}$). The results from profile and profile slopes comparisons are summarized in Table 1 according to layers.

### 4.2 PROPAGATION DATA

An independent evaluation of the bulk-models versus direct-measured profiles compares observed versus predicted propagation with the predicted based on both direct and bulk model derived profiles. Two antennas at different heights above the surface transmitted radio waves at three frequencies, S-Band (2.975 GHz), X-Band (9.7 GHz) and Ku-Band (17.7 GHz), Anderson et al. (2003). The transmitting antennas were aboard R/P FLIP and at nominal heights above sea level of 12.62 and 4.88 meters. The receiving antenna was on shore, 25.77 km away, at a nominal height above sea level of 4.73 meters. The 5-minute cyclic propagation data were averaged over the five-minute collection periods yielding averaged values for each frequency/antenna height combination every thirty minutes.

Figs. 11 through 16 show comparisons between predicted propagation loss and measured values for the different frequencies and antenna heights. These figures show that propagation predictions based on the smoothed profiles from merged kite-sonde and buoy data are much more variable than either the propagation measurements or the propagation predictions based on bulk profiles. For S-Band (Figs. 11 and 12) bulk profiles produced consistently low predictions of propagation loss, but were able to capture some of the variability of the measurements. The merged profiles showed much less skill in predicting propagation loss. For the X-Band (Figs. 13 and 14) the bulk profiles showed forecast skill only for the high antenna. Both types of profiles had poor propagation loss predictions for the low antenna in the X-Band. For the Ku-Band (Figs. 15 and 16) the bulk profile propagation loss predictions show a modest increase as propagation loss increased. With the exception of two outliers, Ku-band results in Fig. 15 show that the merged profiles provide relatively better predictions of propagation loss compared to the bulk profile predictions, but were still marginal. The Ku-band low antenna results in Fig. 16 indicate that neither the observed nor bulk model profiles adequately predicted the propagation loss.

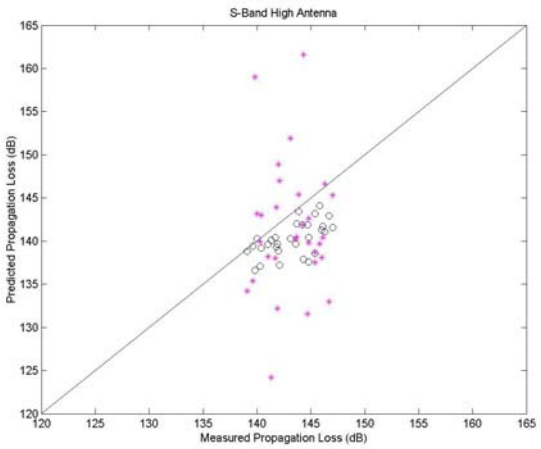


**Figure 11.** Predicted versus measured propagation loss for the S-Band high antenna. Black circles are bulk predictions, magenta asterisks are merged kite/buoy predictions.

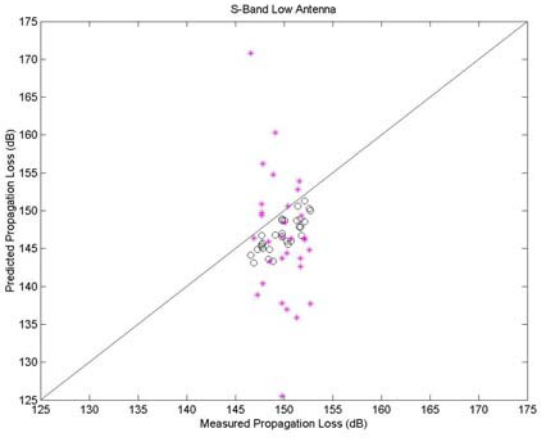


**Figure 12.** As above, but for the S-Band low antenna.

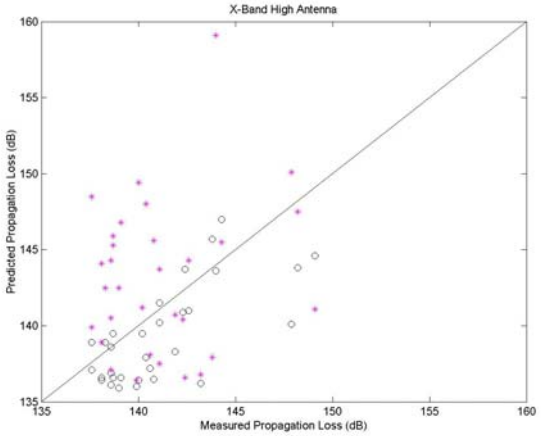


**Figure 13.** As above, but for the X-Band high antenna.

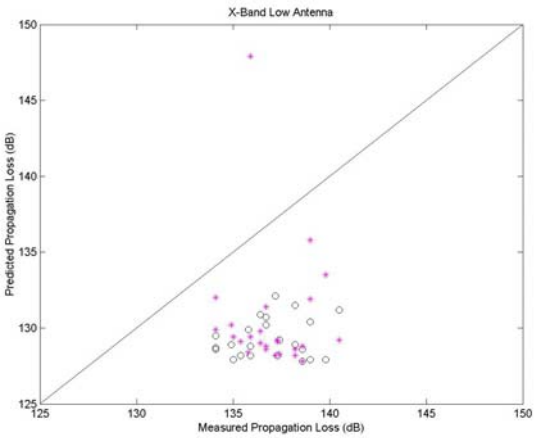


**Figure 14.** As above, but for the X-Band low antenna.

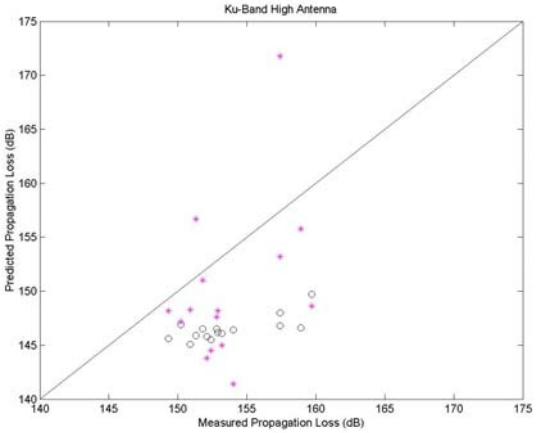


**Figure 15.** As above, but for the Ku-Band high antenna.

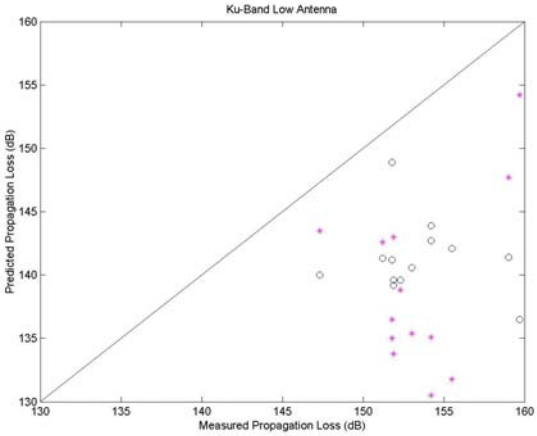


**Figure 16.** As above, but for the Ku-Band low antenna.

## 5. CONCLUSIONS

Conclusions from this preliminary interpretation relate to how the bulk model was able to describe the merged kite-buoy profiles and the resulting impact on RF propagation prediction.

### 5.1 *Profiles of Modified Refractivity*

The gradients of modified refractivity determined using bulk methods and obtained from direct measurement (using data from kite-borne radiosondes merged with buoy data) showed good agreement above 3.5 meters. Between 3.5 meters and ten centimeters, the buoy-based profile data indicates that the humidity gradient is stronger than that predicted by the bulk methods, leading to a stronger gradient of modified refractivity. Reasons for this disagreement will be the subject of future analyses with more complete data obtained during RED, including the 2-dimensional wave data.

### 5.2 *Propagation Predictions*

Propagation predictions based on smoothed profiles of direct (merged) measurements of modified refractivity show much more variability than predictions based on profiles generated using bulk methods for all frequencies. Propagation predictions based on smoothed profiles of direct measurements of modified refractivity show much less correlation with measured propagation at any frequency. In the S-Band (and for the X-Band transmitted from the higher antenna), propagation predictions based on bulk profiles had reasonable correlation with measured propagation. It is believed that the possible profile features causing these discrepancies could be further investigated by using AREPS to generate propagation predictions for environmental profiles that slowly varied from a bulk shape to a merged shape.

## REFERENCES


Anderson, K. D., P. A. Frederickson, and E. Terrill, 2003: Air-Sea Interaction Effects on Microwave Propagation over the Sea during the Rough Evaporation Duct (RED) Experiment. **Proceedings, 12th Conference on Interaction of the Sea and Atmosphere,** 9–13 February 2003, Long Beach, CA.

Fairall, C. W., E. F. Bradley, D. P. Rogers, J. B. Edson, and G. S. Young, 1996; Bulk Parameterization of Air-Sea Fluxes for Tropical Ocean-Global Atmosphere Coupled-Ocean Atmosphere Response Experiment. *Journal of Geophysical Research*, **101**, No. C2, 3747-3764.

Frederickson, P. A., K. L. Davidson, K. Anderson, S. Doss-Hammel, and D. Tsintikidis, 2003: Air-Sea interaction Processes observed from buoy and propagation measurements during the RED Experiment. **Proceedings, 12th Conference on Interaction of the Sea and Atmosphere,** 9–13 February 2003, Long Beach, CA

Henson, R., 2002; How Dry They Are: Public-Private Team Fixes Sounding Bias. *UCAR Quarterly*, Spring 2002, 6.

Mabey, D. L., 2002; Variability of Refractivity in the Surface Layer: RED Buoy/Kite Profiles. Naval Postgraduate School M.S. Thesis, June 2002, 45 pp.


**Table 1.** Mean and standard deviation of the differences of both the actual values of modified refractivity and the gradients of modified refractivity between the bulk and smoothed profiles, based on 45 averaging periods. The information in the two right-hand columns is that presented in Fig. 10.

| | $M_{bulk}$-$M_{smoothed}$ | | $dM/dz_{bulk}$-$dM/dz_{smoothed}$ | |
|---|---|---|---|---|
| | Mean | Std | Mean | Std |
| $z < 0.1$ m | -0.0317 | 0.0508 | -125 | 18.9 |
| $0.1 \text{ m} \leq z < 1$ m | -5.24 | 1.28 | 11.9 | 1.76 |
| $1 \text{ m} \leq z < 3.5$ m | -0.548 | 0.423 | 0.711 | 0.284 |
| $3.5 \text{ m} \leq z < 5$ m | 0.110 | 0.444 | 0.122 | 0.168 |
| $5 \text{ m} \leq z < 12.4$ m | 0.320 | 1.02 | 0.0230 | 0.126 |
| $12.4 \text{ m} \leq z < 50$ m | 0.194 | 2.11 | -0.00924 | 0.0355 |